Contents

Part I
Trends in Traditional Inorganic Materials

Chapter 1
Investigating the Performance of Bismuth-Antimony Telluride

Zinovi Dashevsky and Sergey Skipidarov

Abstract We provide the rationale for possible significant improving efficiency of low-temperature thermoelectric generators (TEGs) based on bismuth-antimony telluride $(Bi_2Te_3)_x(Sb_2Te_3)_{1-x}$ ternary alloys.

It has been shown by experiments that using in TEGs of *p*-type legs made of $(Bi_2Te_3)_x(Sb_2Te_3)_{1-x}$ material with orientation alternative to traditional, i.e., when cleavage planes of legs are transverse to heat flux direction, results in increasing in thermoelectric efficiency by an average of 25% in the temperature range from 100 °C to 350 °C.

1.1 Introduction

Development and wide application of thermoelectric generation as user-friendly direct energy conversion technology are limited mainly by two factors:

- Relatively low conversion efficiency of thermoelectric generators (TEGs)
- Limited resources of thermoelectric materials for large-scale production of high-performance TEGs for industrial applications

Researchers and engineers focus their efforts on solving these problems by:

- Increasing in thermoelectric efficiency Z in a wide range of operating temperatures 50–1000 °C
- Research and development activity and arranging production of novel high-performance thermoelectric materials consisting of elements which are in abundance on the Earth

Unfortunately, situation with candidates for new high-performance materials is far from satisfactory: there are some potential effective candidates for using in mid-temperature range (300–550 °C), but there are no currently high-performance candidates for low-temperature range (below 300 °C) which are able to replace

Z. Dashevsky · S. Skipidarov (✉)
RusTec LLC, Moscow, Russia
e-mail: skipidarov@rustec-msk.com

S. Skipidarov, M. Nikitin (eds.), *Novel Thermoelectric Materials and Device Design Concepts*, https://doi.org/10.1007/978-3-030-12057-3_1

traditional materials based on bismuth-antimony telluride $(Bi_2Te_3)_x(Sb_2Te_3)_{1-x}$ ternary alloy. The main problem is high content of deficit tellurium in these materials reaching about 50%. There are no deposits of tellurium ores in the Earth; tellurium is extracted as a by-product in the production of copper. From one side, consumption of tellurium in industry is low, but from another side, due to low content in the Earth, production volume of tellurium is very limited. Till so far, tellurium has been used as doping additive in alloy steel production. However, production of solar photovoltaic (PV) panels based on CdTe began recently, and, if production will grow in the near future, then affordability of tellurium will be a serious challenge for thermoelectric applications, due to both possible sharp rise in tellurium prices and shortage on the market.

It all stimulates research works for increasing in thermoelectric efficiency of well-known bismuth and antimony chalcogenides that, albeit indirectly, can reduce the consumption of tellurium.

We will consider evident, but nontrivial, approach of improving the efficiency of low-temperature thermoelectric *p*-type $(Bi_2Te_3)_x(Sb_2Te_3)_{1-x}$ ternary alloys. We made a choice on *p*-type materials deliberately. If new effective tellurium-free thermoelectric materials will be discovered, then, likely, those will be *n*-type materials, and *p*-type thermoelectric materials available now will be irreplaceable for a long time. It's because electron mobility μ_e in conduction band of semiconductor materials (Si, Ge, GaAs, etc.) is practically always much higher than heavy hole mobility μ_h in valence band in entire reasonable temperature range. And, as the result, thermoelectric efficiency, which is proportional to mobility of major charge carriers, should generally be higher in materials of *n*-type legs (major charge carriers are electrons) than in materials of *p*-type legs (major charge carriers are heavy holes).

In addition, lower heavy hole mobility in comparison with electron mobility should cause a sharp drop of Z value of *p*-type legs with an increase in temperature and approach to intrinsic conductivity when contributions of holes and electrons to total conductivity value become comparable. It is well known that sign of Seebeck coefficient is positive for holes and negative for electrons. Therefore, thermal generation of electrons in *p*-type material, even in low concentration, will sharply decrease in total value of Seebeck coefficient, which, eventually, tends to zero as the concentration of minority charge carriers (electrons) increases.

The structures of the valence and the conduction bands of $(Bi_2Te_3)_x(Sb_2Te_3)_{1-x}$ ternary alloys are practically similar (that is an essential advantage) which provides highly competitive and unrivaled performance till so far.

1.2 Selection Criteria of Effective Thermoelectric Material

A.F. Ioffe has stated selection criteria of effective thermoelectric material as "the material with the electrical conductivity like a good metal and the thermal conductivity like good isolator." A.F. Ioffe deserves a full credit for understanding that,

namely, "middle" class of materials, semiconductors can provide the best thermoelectric performance as thermoelectric materials.

The conversion efficiency of heat energy to electric power depends on figure of merit of thermoelectric material—factor Z, which is expressed as:

$$Z = \frac{S^2\sigma}{\kappa}, \tag{1.1}$$

where S is Seebeck coefficient, σ is electrical conductivity, and κ is thermal conductivity of thermoelectric material.

At acoustic phonon scattering of charge carriers (charge carrier's mean free path $l = l_0 E^{\mathrm{r}}$, where l_0 is constant, E is charge carrier energy, and scattering parameter $r = 0$), Seebeck coefficient is written as:

$$S = \frac{k_0}{e}\left[2\frac{F_1(\mu^*)}{F_0(\mu^*)} - \mu^*\right], \tag{1.2}$$

where k_0 is Boltzmann constant, e is electron charge, F_{i} are Fermi integrals, and μ^* is reduced Fermi level (for conduction band $\mu^* = \frac{E_{\mathrm{c}} - E_{\mathrm{F}}}{k_0 T}$, E_{c} is the bottom of conduction band and E_{F} is Fermi level; for valence band $\mu^* = \frac{E_{\mathrm{F}} - E_{\mathrm{v}}}{k_0 T}$, E_{v} is the top of valence band).

The electrical conductivity σ of a semiconductor with concentration of charge carriers $n(p)$ is given by well-known formula:

$$\sigma = en(p)\mu_n(\mu_p), \tag{1.3}$$

where $n(p)$ and $\mu_n(\mu_p)$ are electron (hole) concentration and mobility. Electron concentration in the conduction band is determined by expression:

$$n = 4\pi\frac{\left(2m_n^* k_0 T\right)^{3/2}}{h^2}F_{1/2}(\mu^*), \tag{1.4}$$

where m_n^* is the density of states (DOS) effective mass of electrons, and in the case of many-ellipsoid (N) model, it is defined as:

$$m_n^* = N^{2/3}(m_1 m_2 m_3)^{1/3}, \tag{1.5}$$

where m_1, m_2, m_3 are the components of effective mass along the main axis of ellipsoids.

The hole concentrations in the valence band are determined by expression:

$$p = 4\pi\frac{\left(2m_p^* k_0 T\right)^{3/2}}{h^2}F_{1/2}(\mu^*), \tag{1.6}$$

where m_p^* is the density of states (DOS) effective mass of heavy holes. The mobility in a semiconductor with a simple parabolic band is written as:

$$\mu = e\tau/m_c^*, \tag{1.7}$$

where τ is the average pulse relaxation time (the time defining a mean free path) and m_c^* is effective mass of charge carrier.

Heat transport is determined by total thermal conductivity κ of semiconductor which consists of three components—lattice thermal conductivity κ_L by phonons, electronic thermal conductivity κ_e by free electrons or holes, and ambipolar thermal conductivity κ_a by electron-hole pairs in the intrinsic conduction region:

$$\kappa = \kappa_L + \kappa_e + \kappa_a. \tag{1.8}$$

The heat transport by elementary excitations (phonons) can be described by formula:

$$\kappa_L = \frac{1}{3} C_v \nu^3, \tag{1.9}$$

where C_v is the specific heat at constant volume and ν is the velocity of propagation of elementary excitation.

Electronic thermal conductivity can be described by Wiedemann-Franz law:

$$\kappa_e = L_0 \sigma T, \tag{1.10}$$

where L_0 is constant known as Lorenz number. For scattering by the acoustic phonons, Lorenz number is given by:

$$L_0 = 2\left(\frac{k_0}{e}\right)^2. \tag{1.11}$$

Seebeck coefficient S decreases with a growth of charge carriers concentration $n(p)$, and in a metal with charge carriers concentration $\sim 10^{22}$ cm^{-3}, S is close to zero. At the same time, electrical conductivity σ increases with growing concentration of charge carriers $n(p)$. Therefore, dependence of product $S^2\sigma$ as a function of Fermi level E_F has the bell-shaped form. The maximum $S^2\sigma$ is achieved when E_F is close to the bottom of conduction band for n-type semiconductor or close to the top of valence band for p-type semiconductor. In this case, the value of Seebeck coefficient $S \approx 180 \pm 10$ μV/K and concentration $n(p) \sim 5 \times 10^{19}$ cm^{-3}. At concentration $n(p) \sim 5 \times 10^{19}$ cm^{-3}, heat transport is determined mainly by lattice thermal conductivity κ_L through phonons. For optimal concentration of charge carriers (reduced Fermi level $\mu^* \approx 0$), the figure of merit Z practically depends on three parameters:

$$Z \sim \left(m_n^*\right)^{3/2}(\mu/\kappa_L). \tag{1.12}$$

Now we can formulate the selection criteria of the effective thermoelectric material:

1. Semiconductor material (elemental, compound, alloy, composite, multilayer, superlattice, low-dimensional) should preferably consist of heavy atoms; it will cause a low frequency of thermal vibrations of lattice and, properly, significant decrease in lattice thermal conductivity κ_L.
2. Semiconductor material should have high dielectric constant $\varepsilon \geq 100$, that reduces significantly the scattering of charge carriers by impurity ions, and small effective mass of major charge carriers (m_n^* of electrons for n-type and m_p^* of heavy holes for p-type). These two criteria provide high mobility of charge carriers μ.

   Note that high dielectric constant ε leads to decrease in ionization energy of the impurity atoms (which is practically approaching zero). As a result, energy level of impurity merges with the conduction or valence band, and concentration of electrons in the conduction band of n-type material or concentration of heavy holes in the valence band of p-type material becomes constant (similar to metal) and equals to dopant concentration in temperature range from 0 K to the onset of intrinsic conductivity.
3. Semiconductor material should have multi-valley structure of the conduction band for n-type and the same structure of the valence band for p-type. In this case, concentration of charge carriers increases many times without changing energy of Fermi level E_F, because it is simply proportional to the number of ellipsoids and, properly, the electrical conductivity σ rises seriously as well.
4. Semiconductor material should allow heavy doping with impurities, ensuring the achievement of high concentrations of charge carriers $n(p) \geq 10^{19}$ cm^{-3} that will result in optimal Fermi level energy E_F, and, having in mind maximum value of $S^2\sigma$, it will mean $(E_F - E_c) \sim 0$ eV for n-type and $(E_v - E_F) \sim 0$ eV for p-type.
5. Bandgap of semiconductor E_g in operating temperature range of thermoelectric material should be $E_g \geq 8k_0T$, to minimize contribution of thermally generated minority charge carriers to total electrical conductivity, leading to decrease in thermoelectric efficiency.

1.3 Basic Properties of Thermoelectric Materials Based on Bismuth Telluride

Bismuth telluride Bi_2Te_3 consists of heavy atoms; that is one of the reasons for its high thermoelectric efficiency. Crystal structure of Bi_2Te_3 (Fig. 1.1, left) is characterized by rhombohedral actual primitive cell (Fig. 1.1, top right). Lattice constant c of the rhombohedral cell (between bottom and top points) equals to approximately 5.08 nm. This is maximal size of cell which is the actual measure for comparison

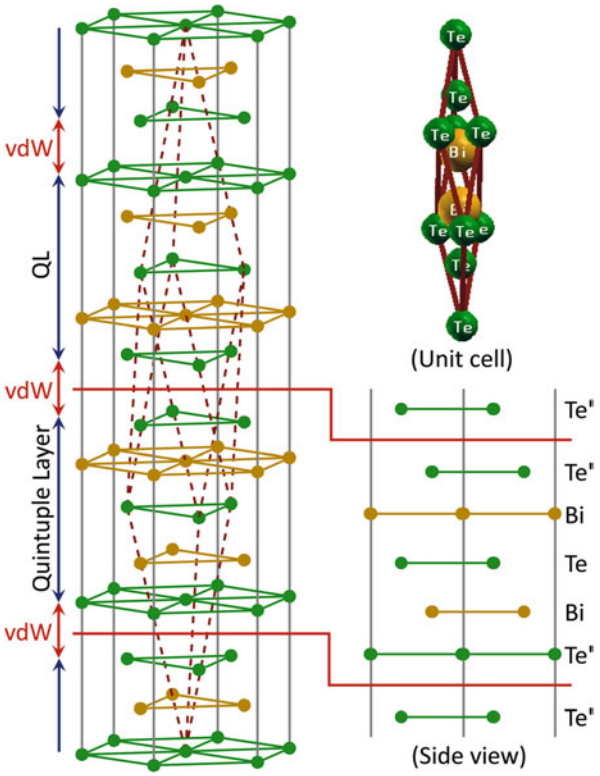

Fig. 1.1 (Left) Crystal structure of Bi_2Te_3 with rhombohedral unit cell embedded inside. Bismuth and tellurium atoms are shown as yellow and green circles, respectively. (Top right) A separate rhombohedral unit cell structure, generated from XCrySDen. (Bottom right) Side view of a quintuple layer QL ($Te' - Bi - Te - Bi - Te'$) with each layer separated from the next by the real-ratio distance. The superscripts are used to distinguish two types of differently bonded Te atoms [1]

with size of nanoparticles when we will consider nanotechnology approaches. The bulk structure consists of orderly stacked alternating hexagonal monatomic crystal planes. Stacks of five neighboring monoatomic layers $Te' - Bi - Te - Bi - Te'$ form quintuple layers (QLs) (Fig. 1.1, bottom right). Bonding between atomic planes within a QL is strong covalent with a small fraction of ionic bonding. Ionic bond component is explained by different valence of Te (6) and Bi (5). The outer adjacent atomic layers of QLs are attracted by weak van der Waals (vdW) forces. This weak vdW bonding between QLs allows the crystal to be easily cleaved along an inter-QL plane (vdW interface), so crystals of Bi_2Te_3 have clearly defined cleavage planes. For convenience, crystal structure of Bi_2Te_3 and related alloys is often considered in the hexagonal basis. A unit cell in the hexagonal basis contains three QLs; lattice constant c equals to 3.049 nm.

As already mentioned, Z is determined by the ratio of the mobility of charge carriers to lattice thermal conductivity. Let's consider the case when the mobility is determined by scattering of charge carriers due to thermal vibrations of lattice only. It should be understood here that electrons or holes are scattered not by thermal vibrations of the atoms but by electric fields which occur due to distortion of crystal periodic potential because of these vibrations. The stronger the distortion of the

periodic potential, the higher is the intensity of local fields caused by thermal vibrations. Therefore, mobility of charge carriers is usually low in ionic crystals, where relief of crystal potential is most pronounced. In contrast, in crystals with predominant covalent bonds, the crystal potential is smooth (in this case, there is no alternation of positively and negatively charged ions), and the mobility of charge carriers is much higher. As for lattice thermal conductivity, bismuth telluride consists of heavy Bi and Te atoms that cause a low frequency of thermal vibrations of lattice and, properly, a low lattice thermal conductivity. Basic parameters of Bi_2Te_3 are given in Table 1.1.

Specific crystalline structure of Bi_2Te_3 semiconductor gives in the result strong anisotropy of basic properties. As a result, values of electric and thermal conductivity in direction parallel to cleavage planes are much higher than transverse values (Table 1.1). Van der Waals (vdW) interfaces between quintuple outer adjacent atomic layers play a significant role in forming anisotropy of electric and thermal conductivity (Fig. 1.2) [1].

Table 1.1 Basic properties of bismuth telluride [2]

	Parameter	Symbol	Value
1	Melting point	T_m	585 °C
2	Bandgap at 300 K	E_g	0.13 eV
3	Temperature dependence of bandgap	dE_g/dT	-9×10^{-5} eV/K
4	Debye temperature	T_D	155.5 K
5	Number of ellipsoids:		
	– Valence band	N_c	6
	– Conduction band	N_v	6
6	Density of states (DOS) effective mass:		
	– Electrons	m_n^*	0.45 m_0
	– Heavy holes	m_p^*	0.69 m_0
7	Mobility of charge carriers:		
	– Electrons	μ_e	1200 $cm^2/(V \times s)$
	– Heavy holes	μ_p	510 $cm^2/(V \times s)$
8	Temperature dependence of mobility:		
	– Electrons	$d\mu_e/dT$	$T^{-1.7}$
	– Heavy holes	$d\mu_p/dT$	$T^{-2.0}$
9	Scattering parameter:		
	– Electrons	r_e	0
	– Holes	r_p	0
10	Dielectric constant	ε_0	400
11	Concentration of charge carriers at 300 K	n_i	10^{18} cm^{-3}
12	Lattice thermal conductivity along cleavage planes	$\kappa^{\parallel}$	14.5×10^{-3} W/(cm × K)
13	Anisotropy of thermal conductivity	$\kappa^{\parallel}/\kappa^{\perp}$	~2–3
14	Anisotropy of electrical conductivity:		
	n-type	$(\sigma^{\parallel}/\sigma^{\perp})_n$	4–6
	p-type	$(\sigma^{\parallel}/\sigma^{\perp})_p$	2.7

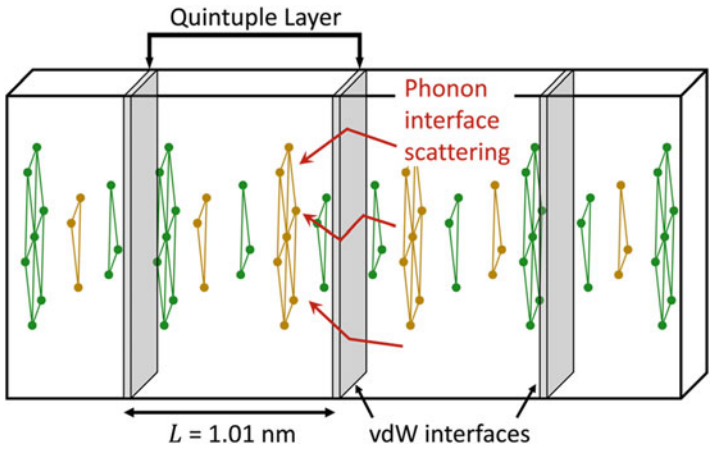

Fig. 1.2 Bi_2Te_3 structure projected in a superlattice structure. Van der Waals (vdW) interfaces exist between quintuple layers and cause an additional anharmonic phonon scattering [1]

Isotropy is fundamental property of Seebeck coefficient S in crystals having Bi_2Te_3 structure with charge carriers of one sign only. Therefore, as follows from Table 1.1 and Formula (1.12), anisotropy of Z of n-type material is high and close to 2, whereas Z of p-type material is almost isotropic. In crystals with anisotropic mobility of charge carriers like Bi_2Te_3, Seebeck coefficient becomes also anisotropic in the presence of charge carriers of opposite sign, especially when contribution of that charge carriers to total electric conductivity becomes tangible.

A.F. Ioffe suggested an idea of improving thermoelectric efficiency of available thermoelectric materials—elemental and binary compound semiconductors by means of producing of the so-called solid solutions (first, binary alloys of elemental semiconductors, binary compound semiconductors and ternary alloys of binary compounds). It opened great opportunities for improving efficiency and for Bi_2Te_3 as well.

Approach to development of improved performance ternary alloys based on Bi_2Te_3 was as follows: in bismuth telluride, the bismuth sublattice forms a negative charge; therefore, electrons should scatter on this sublattice, and, respectively, holes should scatter on tellurium sublattice. Thus, to get improved n-type ternary alloys, the third component (e.g., selenium) should be introduced in the tellurium sublattice, and to get improved p-type ternary alloys, the third component (e.g., antimony) should be introduced in the bismuth sublattice.

As a result, n-type $(Bi_2Te_3)_y(Bi_2Se_3)_{1-y}$ ternary alloys have been developed by S.S. Sinani and G.N. Gordeeva [3] in year 1956 and p-type $(Bi_2Te_3)_x(Sb_2Te_3)_{1-x}$ ternary alloys—by G.I. Shmelev [4] in year 1959. And these materials remain unrivaled in thermoelectric efficiency to nowadays.

By the way, the validity of an idea that alloys can provide higher thermoelectric efficiency has been confirmed later when developing high-temperature thermoelectric materials based on Si - Ge alloy system.

As for *p*-type $(Bi_2Te_3)_x(Sb_2Te_3)_{1-x}$ ternary alloys, G.I. Shmelev has determined (during the work on PhD thesis) alloy composition value where ratio μ/κ_L was maximal. Note that thermoelectric efficiency of pristine binary compounds Bi_2Te_3 and Sb_2Te_3 was equal to $Z = 1 \times 10^{-3}$ K^{-1}, whereas efficiency of *p*-type $(Bi_2Te_3)_x(Sb_2Te_3)_{1-x}$ ternary alloy with optimal composition x was equal to $Z = 2.6 \times 10^{-3}$ K^{-1}, which is very close to the best current values $(3.0–3.2) \times 10^{-3}$ K^{-1}.

The increase in thermoelectric efficiency of $(Bi_2Te_3)_x(Sb_2Te_3)_{1-x}$ ternary alloys with growth of Sb_2Te_3 content was due to a decrease in thermal conductivity which reached minimum at content of 70–80 mole % of Sb_2Te_3. In addition, at such content of Sb_2Te_3, ordering of crystal structure of ternary alloy was observed, which caused an increase in mobility of charge carriers. It should be noted that bandgap E_g of $(Bi_2Te_3)_x(Sb_2Te_3)_{1-x}$ ternary alloys increases monotonically with growth of mole fraction of Sb_2Te_3 in alloy, which is very important for thermoelectric generation applications. The bandgap of Bi_2Te_3 is not more than $E_g = 0.13$ eV at 300 K, i.e., $E_g/k_0T = 5$, and with increasing temperature, thermal generation of minority charge carriers degrades sharply thermoelectric efficiency of *p*-type Bi_2Te_3.

We describe and discuss in the chapter possible techniques of suppressing the negative effect of thermally generated minority charge carriers (electrons) on thermoelectric efficiency of *p*-type $(Bi_2Te_3)_x(Sb_2Te_3)_{1-x}$ ternary alloys.

1.4 Manufacturing Technology of Thermoelectric Materials

One of the rigorous selection criteria of semiconductor material for thermoelectric generation applications is mechanical strength, since legs made of that material will operate at significant temperature difference and, hence, at high mechanical stress. Furthermore, considering the tendency to decrease consumption of thermoelectric materials, especially, with high content of deficit tellurium, by means of shortening of legs' height, the role of enhanced mechanical strength is growing, since the thermomechanical stresses in thermoelectric leg increase inversely with the square of the height. Therefore, the use of legs made of materials manufactured by traditional crystallization/melting methods (zone melting technique, Czochralski method, Bridgman method) is unrealistic on practice. Materials for practical use in thermoelectric generation applications are now and will always be of polycrystalline or composite nature.

1.4.1 Pressing Technique

As a rule, serial Bi_2Te_3-based bulk materials are produced with powder compaction by pressing that included synthesis of ingots by proper melting technique, grinding of ingots into powder, pressing, and annealing. Technique enables also to do the so-called co-pressing of *n*- and *p*-type legs, when, during compaction, *n*- and *p*-type legs connect to each other forming ready-made thermocouple. The uniaxial pressing technique provides manufacturing of bulk anisotropic thermoelectric materials with optimal crystallographic texture including ternary alloys of $(Bi_2Te_3)_y(Bi_2Se_3)_{1-y}$ for *n*-type legs and $(Bi_2Te_3)_x(Sb_2Te_3)_{1-x}$ for *p*-type legs.

Thermoelectric efficiency Z of Bi_2Te_3 and related alloys is maximal when heat flow direction is parallel to cleavage planes of material (grain). Therefore, disordered orientation of crystalline grains in pressed materials should reduce Z. In addition, the value of Z can degrade due to defects (grain boundaries, oxide films, dislocations, vacancies, microcracks, etc.) that scatter charge carriers. Inherent feature of thermoelectric Bi_2Te_3 and related alloys manufactured by pressing is some self-ordering of grain orientation when cleavage planes are laying mainly perpendicular to the direction of pressing. This is because, during grinding, the ingot of starting material splits along the cleavage planes, and powder particles take the form of plates in which the plane coincides with the cleavage plane. The preferential orientation of the grains causes anisotropy of the properties of pressed materials: σ, κ, and Z have the greatest values in the direction perpendicular to the direction of pressing. The electrical conductivity and thermal conductivity of pressed samples are less than in polycrystals obtained by crystallization from melt.

1.4.2 Spark Plasma Sintering Technique

SPS (spark plasma sintering) technique of powder compaction became recently a frequent practice but in laboratory only. SPS technique allows of compacting powders made of materials that are difficult to compact by standard pressing due to the need to use forces exceeding the strength of press tool materials. In addition, SPS process provides sintering of grains without significant heating of whole load of powder, which is valuable for compacting not entirely stable systems, e.g., nanostructured powders. High-throughput conveyor-type SPS machines are recently available on the market, which is evidence of transfer of SPS technology for wide use in industry.

1.4.3 Extrusion Technique

Ideally, powder compaction technique of Bi_2Te_3 and related alloys should enable obtaining polycrystalline (textured) ingots (rods) with given orientation, since electrical conductivity and thermal conductivity are anisotropic, especially in *n*-type materials, because of layered structure (Table 1.1). As for *p*-type materials, at first sight, manufacturing of well-textured polycrystalline materials is not so critical for applications, since *Z* value at temperatures up to 100 °C is practically isotropic. But, as it will be shown further, that's all wrong, and obtaining oriented polycrystalline (textured) ingots (rods) is actual task for *p*-type materials.

The presence of evident cleavage planes in Bi_2Te_3 and related alloys provides obtaining of "flakes" during grinding, which, being packed in a mold, enable manufacturing well-textured ingots (rods) during subsequent pressing. This is a decisive point to the use of pressing and SPS techniques for compacting materials based on Bi_2Te_3 and related alloys.

However, materials with even better texture can be manufactured by hot extrusion technique of powder compaction. In this case, cleavage planes of grains align strictly parallel to the axis of extrusion. In addition, plastic deformation of material under high hydrostatic pressure provides effective repairing of structural defects and obtaining polycrystalline ingots (rods) with grain size about 10 μm and density above 96% of single crystal one.

At present time, hot extrusion becomes the main industrial technology for manufacturing high-performance Bi_2Te_3 and related alloy materials. Ingots (rods) of extruded materials with a diameter of up to 30 mm and thermoelectric efficiency at 25 °C $Z = (3.1–3.2) \times 10^{-3}$ K^{-1} for *p*-type material and $Z = 2.9 \times 10^{-3}$ K^{-1} for *n*-type material are commercially available (data provided by RusTec LLC, www.rustec-msk.com).

1.5 Options for Improving Efficiency of Thermoelectric Materials

Growing interest in "green energy" and requirement to reduce atmospheric greenhouse gas emissions under Kyoto Protocol stimulated formation of state R&D programs in the field of prospective thermoelectric materials and generators in several countries. Inflow of investments led to involvement of many new researchers in solving different thermoelectric issues, and now research work in thermoelectricity is one of the most active. Much research work is being done for improving thermoelectric efficiency *Z* of known and novel thermoelectric materials. Different approaches are being studied for that. However, there are not yet tangible results concerned improving *Z* value of well-known high-performance low-temperature materials Bi_2Te_3 and related alloys. Improving *Z* has only been shown in materials with initial low *Z* value. For example, significant progress in improving efficiency of

mid-temperature thermoelectric materials—skutterudites—led to increase in Z values which are now close to real use in industry. Skutterudite materials were known for a long time, e.g., $CoSb_3$ was discovered by L.D. Dudkin in year 1956 and described in his PhD work [5].

There is no progress in improving thermoelectric efficiency of low-temperature materials for more than 60 years. The value of $Z = 3 \times 10^{-3}$ K^{-1} remains an unbeaten record, and new approaches and solutions are needed to overcome it.

1.5.1 Nanotechnology and Low-Dimensional Structures

Progress in grinding equipment is evident. High-speed planetary ball mills are commercially available now. Idea to decreasing thermal conductivity and, hence, increasing Z by reducing size of grains with proper increase in the number of boundaries which scatter phonons has become actual again. Let's consider this option more detailed. To provide a marked increase in scattering of phonons, grain sizes should be comparable to mean free path of phonons which equals to about 15 nm in materials like $(Bi_2Te_3)_x(Sb_2Te_3)_{1-x}$. At the same time, crystal structure of Bi_2Te_3 is rhombohedral cell with lattice constant c equals to approximately 5.08 nm (Sect. 1.3). It seems to be difficult to fabricate materials like Bi_2Te_3 with grain sizes that are only three times of the size of crystal unit cell using ordinary grinding of an already crystallized material. Likely, approach could be realized for densely packed cubic materials such as PbTe. And, although researchers have already published reports about successes of increase in Z of nanostructured $(Bi_2Te_3)_x(Sb_2Te_3)_{1-x}$, manufacturers of thermoelectric devices have not yet presented clear evidences that it's so.

It should be noted that the idea of increasing in thermoelectric efficiency by using structures with higher number of grain boundaries for phonon scattering and with barrier effect that provides increase in average energy of charge carriers in flow has always been in sight of researchers. It was found that increasing in thermoelectric efficiency was observed mainly for p-type $(Bi_2Te_3)_x(Sb_2Te_3)_{1-x}$ ternary alloys and no noticeable increase was observed in n-type $(Bi_2Te_3)_y(Bi_2Se_3)_{1-y}$ ternary alloys, and it was concluded that grain boundaries scatter electrons more strongly than holes. Gain in thermoelectric efficiency due to effects associated with grain boundaries did not exceed a few percent.

In contrast to methods of fabricating nanoparticles by grinding of a crystallized material with already formed chemical bonds, M.V. Kovalenko and colleagues [6–9] proposed original approach to building nanoparticles of thermoelectric materials from atoms by liquid-phase synthesis without melting. In proposed method, synthesis of nanoparticles occurs in aqueous solutions through the proper precursors. This approach allows to configure internal structure of nanoparticles, i.e., technology could produce structured materials both with effective scattering of charge carriers on phonons and with transformation of energy spectrum, including changes of effective mass of density of states (DOS) which is one of the key parameters for

thermoelectricity. Apparent advantages of this technology in comparison with traditional vapor-phase technology are flexibility, ease in scaling, and low cost of technological processes.

Obviously, manufacturing of high-performance nanomaterials by compaction of nanoparticles will require solving of difficult problems including building a perfect texture of anisotropic materials like Bi_2Te_3, as well as ensuring reliable encapsulation of nanoparticles to prevent oxidation, aggregation, and crystallization at high temperatures in running thermoelectric generators.

Theoretical work published in year 1993 by L.D. Hicks and M.S. Dresselhaus [10] can be considered as kickoff for nanoengineering in thermoelectricity. Under certain assumptions made, it was shown that the reduction in body size in one or a few dimensions to nanometer level can cause due to quantum effects a change of energy spectrum. In transition to low-dimensional structures, the density of states (DOS) changes very strongly. Two key parameters for thermoelectricity—effective mass of charge carriers and Z—depend directly on DOS. Low-dimensional structures are called "quantum well" (2D), "quantum wire" (1D), and "quantum dot" (0D).

Estimations of low-dimensional effects for Bi_2Te_3 done in framework of L.D. Hicks and M.S. Dresselhaus model showed a strong increase in Z when the characteristic size of material grain decreased to 50 Å.

Unfortunately, theory has not yet tested, but development of nanotechnology in thermoelectricity will clear up the matters.

1.6 Novel Thermocouple Made of "Old" Materials

When we speak about options of increasing in efficiency Z, we should keep in mind, first, thermoelectric material operates in generator application over a wide range of temperatures and, second, material which is optimal, e.g., for use in low-temperature range, may be inefficient at higher temperatures. One option to provide optimal (the highest possible) efficiency of thermoelectric leg in wide temperature range is using a leg composed of a few parts (sub-legs) made of several materials with optimal efficiency in specified temperature range. Another option of optimization should also be considered, namely, leg composed of sub-legs made of same material with different crystalline orientation.

Traditionally, legs made of low-temperature materials like Bi_2Te_3 and related alloys are diced out so that cleavage planes in the legs are oriented parallel to heat flux direction. This approach is fully justified for legs made of n-type material, where anisotropy of electrical conductivity is close to 2, since this orientation provides maximum efficiency. However, for p-type legs, this condition is optional. Indeed, when cleavage planes in p-type legs are oriented parallel to heat flux direction, then at room temperature, thermoelectric efficiency of p-type legs is only somewhat ($\sim$ 10%) higher than transverse. The rise in temperature induces thermal generation of minority charge carriers (electrons) with high mobility. Thermally generated

electrons produce an electromotive force of opposite sign that reduces the overall Seebeck coefficient S in accordance with formula:

$$S = \frac{S_n\sigma_n + S_p\sigma_p}{\sigma_n + \sigma_p}, \tag{1.13}$$

where indexes n and p describe parameters determined by electrons and holes, respectively.

Table 1.1 shows that electron mobility is higher than hole mobility and electron concentration increases exponentially with temperature, which leads to a sharp decrease in Seebeck coefficient S and even greater decrease in Z, because Z is proportional to the square of S.

Note that isotropy is a fundamental property of Seebeck coefficient in crystal of any kind of structure with charge carriers of same sign only. As it follows from Formula (1.13), in crystals with anisotropy of charge carrier mobility, Seebeck coefficient becomes also anisotropic in the presence of charge carriers of opposite sign. Therefore, negative effect of minority charge carriers can be minimized by using crystal with orientation parallel to axis with minimal mobility of minority charge carriers. Electron mobility in Bi_2Te_3 and related alloys is minimal in direction transverse to cleavage planes. So, to build highly effective thermocouple operating in the temperature range where intrinsic conductivity began, we should use p-type leg with orientation transverse to cleavage planes. Certainly, n-type legs are diced out always with orientation parallel to cleavage planes, since anisotropy of Z in n-type material is high and close to 2.

However, traditionally, thermoelectric generation modules are assembled of n-type and p-type legs diced out with the same orientation parallel to cleavage planes. Old tradition is not always good tradition.

Temperature dependence of the anisotropy of Z in p-type $Bi_{0.5}Sb_{1.5}Te$ ternary alloy has been studied on two samples with sizes ($L \times W \times H$) 18 mm × 10 mm × 10 mm. Ingot of material has been manufactured by hot extrusion technique (see Sect. 1.4.3). Samples were diced out parallel (i.e., with orientation parallel to cleavage planes) and transverse (i.e., with orientation transverse to cleavage planes) to extrusion axis from an ingot of material with $\sigma = 1850\ \mathrm{Ohm}^{-1} \times \mathrm{cm}^{-1}$ and $S = 157\ \mu\mathrm{V/K}$ at room temperature. Specific electric conductivity σ, Seebeck coefficient S, and specific thermal conductivity κ have been measured in temperature range of 50–380 °C. Figures 1.3, 1.4, and 1.5 show obtained temperature dependences, where indexes ($\|$) and ($\perp$) indicate the kinetic coefficients measured on samples diced out parallel and transverse to the extrusion axis, i.e., parallel and transverse to cleavage planes. Figure 1.6 shows calculated value of Z. Figures 1.7 and 1.8 show temperature dependences of the anisotropy of Seebeck coefficient $S_\perp/S_\|$ and thermoelectric efficiency $Z_\perp/Z_\|$. Obtained results confirm concept that variation of S and Z with growth of temperature is noticeably different in samples with working axis along and transverse to cleavage planes. Impressive gain due to change of the working axis of p-type material from traditional

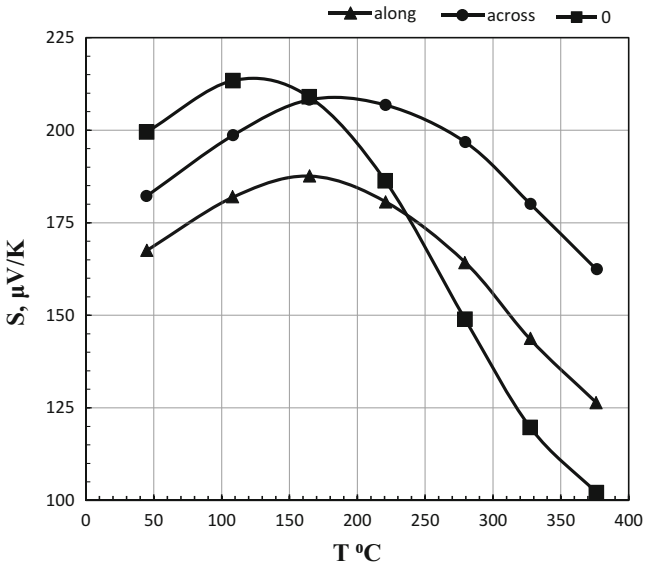

Fig. 1.3 Seebeck coefficient as a function of temperature

Fig. 1.4 Electrical conductivity as a function of temperature

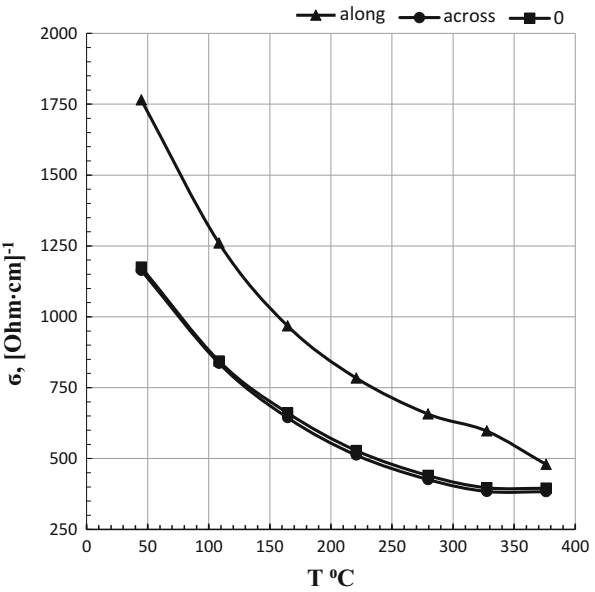

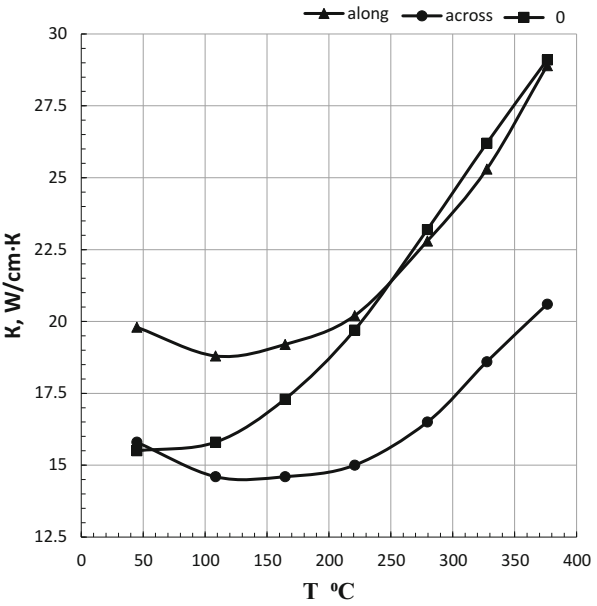

Fig. 1.5 Thermal conductivity as a function of temperature

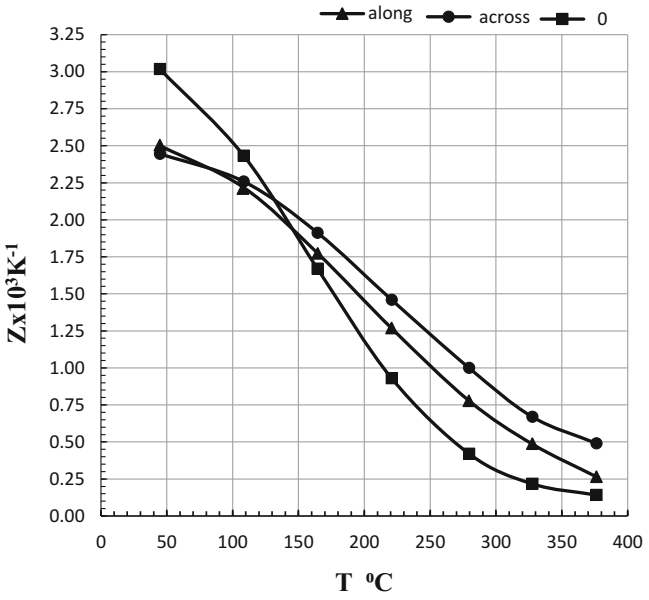

Fig. 1.6 Figure of merit as a function of temperature

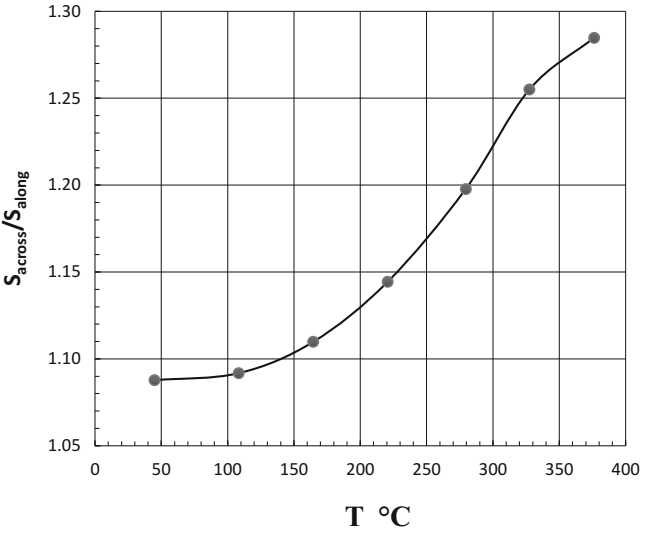

Fig. 1.7 Anisotropy of Seebeck coefficient $S_{\perp}/S_{\parallel}$ as a function of temperature

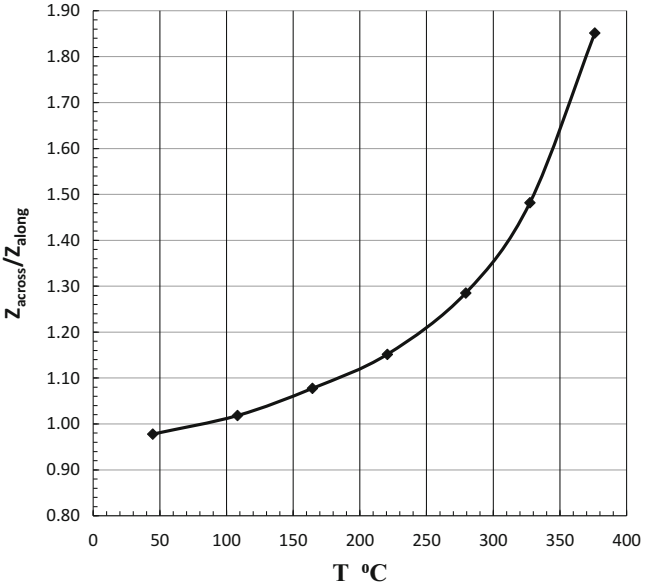

Fig. 1.8 Anisotropy of figure of merit $Z_{\perp}/Z_{\parallel}$ as a function of temperature

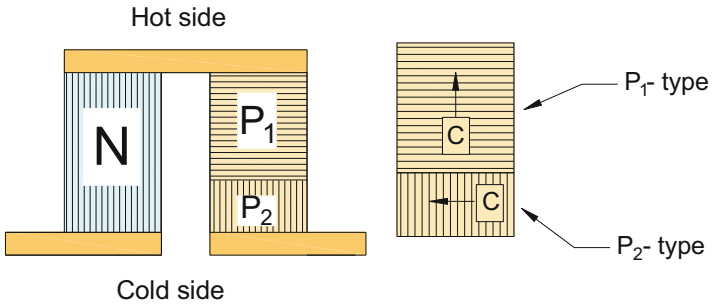

Fig. 1.9 Schematic view of thermocouple with combined *p*-type leg

to alternative reaches at 350 °C up to 50%. That gain in thermoelectric efficiency can easily be obtained on already known materials.

Figures 1.3, 1.4, 1.5, and 1.6 show also temperature dependences (marked "0") of the same kinetic coefficients measured on sample of *p*-type $Bi_{0.5}Sb_{1.5}Te$ material but with lower level of doping and characterized by $\sigma = 1270\ \text{Ohm}^{-1} \times \text{cm}^{-1}$ and $S = 183\ \mu\text{V/K}$ at room temperature. This material with lower level of doping has been optimized for operating temperatures from room temperature and above.

Figure 1.9 suggests optimal design of advanced thermocouple with *p*-type leg composed of sub-legs with mutually perpendicular orientations of crystalline axes. Bottom sub-leg (cold part P_2) for operation in temperature range up to 130–140 °C should be made of moderately doped material ($\sigma \sim 1200\ \text{Ohm}^{-1} \times \text{cm}^{-1}$) with the orientation of working axis parallel to cleavage planes, and top sub-leg (hot part P_1) for higher temperature range should be made of heavily doped material ($\sigma \sim 1800$–-1900 $\text{Ohm}^{-1} \times \text{cm}^{-1}$) with working direction transverse to cleavage planes.

Figure 1.9 shows a sketch of novel thermocouple.

1.7 Conclusions

Clearly expressed anisotropy of Seebeck coefficient *S* in *p*-type $(Bi_2Te_3)_x(Sb_2Te_3)_{1-x}$ ternary alloys at T > 100 °C has been observed for the first time.

Anisotropy of Seebeck coefficient in *p*-type samples with working axis parallel (∥) and transverse (⊥) to cleavage planes arises from anisotropy of mobility of minority charge carriers (electrons) along different crystalline axes $\mu_{\parallel} > \mu_{\perp}$.

At temperatures T > 100 °C, efficiency $Z_{\perp}$ of extruded samples diced out with working axis transverse to cleavage planes is higher than $Z_{\parallel}$ of samples diced out with working axis along cleavage planes. At temperature T = 350 °C, efficiency gain equals to ~1.6.

References

1. K.H. Park, M. Mohamed, Z. Aksamija, U. Ravaioli, Phonon scattering due to van der Waals forces in the lattice thermal conductivity of Bi_2Te_3 thin films. J. Appl. Phys. **117**, 015103 (2015). https://doi.org/10.1063/1.4905294
2. B.M. Goltsman, B.A. Kudinov, I.A. Smirnov, *Thermoelectric semiconductor materials based on Bi_2Te_3* (Nauka, Moscow, 1972)
3. S.S. Sinani, G.N. Gordeeva, Bi_2Te_3—Bi_2Se_3 solid solutions as materials for thermoelements. Tech Phys (Sov.). **26**, 2398–2399 (1956)
4. G.L. Shmelev, Materials for thermoelements based on three-component intermetallic alloys. Solid State Phys (Sov.). **1**, 63–75 (1959)
5. L.D. Dudkin, N.K.H. Abrikosov, Physico-chemical investigations of cobalt antimony. J Inorg Chem (Sov.) **1**, 2096–2101 (1956)
6. M.V. Kovalenko, B. Spokoyny, J.-S. Lee, M. Scheele, A. Weber, S. Perera, D. Landry, D.V. Talapin, Semiconductor nanocrystals functionalized with antimony telluride Zintl ions for nanostructured thermoelectrics. J. Am. Chem. Soc. **32**, 6686–6695 (2010). https://doi.org/10.1021/ja909591x
7. M.V. Kovalenko, L. Manna, A. Cabot, Z. Hens, D.V. Talapin, C.R. Kagan, V.I. Klimov, A.I. Rogach, P. Reiss, D.J. Milliron, P. Guyot-Sionnnest, G. Konstantatos, W.J. Parak, T. Hyeon, B.A. Korgel, C.B. Murray, W. Heiss, Prospects of nanoscience with nanocrystals. ACS Nano **9**, 1012–1057 (2015). https://doi.org/10.1021/nn506223h
8. S. Ortega, M. Ibáñez, Y. Liu, Y. Zhang, M.V. Kovalenko, D. Cadavid, A. Cabot, Bottom-up engineering of thermoelectric nanomaterials and devices from solution processed nanoparticle building blocks. Chem. Soc. Rev. **46**, 3510–3528 (2017). https://doi.org/10.1039/c6cs00567e
9. M. Ibáñez, R. Hasler, Y. Liu, O. Dobrozhan, O. Nazarenko, D. Cadavid, A. Cabot, M.V. Kovalenko, Tuning p-type transport in bottom-up-engineered nanocrystalline Pb chalcogenides using alkali metal chalcogenides as capping ligands. ACS Chem Mater **29**(17), 7093–7097 (2017). https://doi.org/10.1021/acs.chemmater.7b02967
10. L.D. Hicks, M.S. Dresselhaus, Effect of quantum-well structures on the thermoelectric figure of merit. Phys. Rev. B **47**, 12727–12731 (1993)